WATER RESOURCES RESEARCH, VOL. 49, 1099–1106, doi:10.1002/wrcr.20105, 2013

Contribution of mechanical dispersion of vapor to soil evaporation

Jordi Grifoll[1]

Received 18 June 2012; revised 7 January 2013; accepted 10 January 2013; published 28 February 2013.

[1] Conventional methods for numerical simulation of the soil evaporation process do not take into account the mechanical dispersion of vapor in the porous matrix. This omission is due to the uncertainties about the flow process that generates mechanical dispersion and about the numerical value of dispersivity. In this study we assess three processes that can generate mechanical dispersion: (a) temperature variation, (b) barometric pressure variation, and (c) Stefan flow. Order of magnitude estimates show that under natural conditions, only Stefan flow can contribute significantly to the generation of mechanical dispersion. However, a simple sensitivity analysis of the effects of dispersivity on the contribution of different mechanisms to the evaporation process shows that diffusion and mechanical dispersion act in a complementary way. In simulations of a natural system, the evaporation flux increases by only 12% when dispersivity is increased from 0 m (no mechanical dispersion) to 0.078 m, although at the latter value the mechanical dispersion flux contributes up to 40% of the total evaporation flux.

Citation: Grifoll, J. (2013), Contribution of mechanical dispersion of vapor to soil evaporation, *Water Resour. Res.*, *49*, doi:10.1002/wrcr.20105.

1. Introduction

[2] In a narrow subsoil region, close to the soil-atmosphere interface, the transport of liquid water, vapor, and energy determines the evaporation flux. The first formulation for describing water transport under nonisothermal conditions was developed by *Philip and deVries* [1957]. Their model consists of an equation for water transport, in the liquid or vapor phase, and an equation for energy transport. To fit the experimental results to the model predictions, an empirical enhancement factor is applied to the diffusive vapor flux. The Philip and deVries model has been widely accepted and is used in popular simulation environments such as Hydrus-1D [*Šimůnek et al.*, 2008]. However, the meaning of these empirical factors and whether they are strictly necessary are not well documented, and it is possible that the enhancement factor masks transport by other mechanisms. For instance, *Ho and Webb* [1998] argue that available experimental information does not conclusively demonstrate the existence of enhancing mechanisms that would justify the inclusion of enhancement factors. In addition, *Shokri et al.* [2009] show that the coupling between capillary flow and vapor diffusion could be used to estimate vapor flux without enhancement factors.

[3] In this study we analyze the role of mechanical dispersion as a vapor-transport mechanism in natural soil systems. When advection takes place in the gas phase, water vapor is subjected to mechanical dispersion, as is any other species present in the gas phase. However, most mathematical models of nonisothermal evaporation and water transport do not consider mechanical vapor dispersion as an active transport mechanism. One exception is the model used by *Grifoll et al.* [2005], which considers the mechanical dispersion mechanism. The model includes three mass balances and one energy balance. The 1-D mass balances were

$$\frac{\partial \theta_L \rho_L}{\partial t} = -\frac{\partial \rho_L q_L}{\partial z} - f_{LG}, \tag{1a}$$

$$\frac{\partial \theta_G \rho_G}{\partial t} = -\frac{\partial \rho_G q_G}{\partial z} + f_{LG}, \tag{1b}$$

$$\frac{\partial \theta_G \rho_v}{\partial t} = -\frac{\partial}{\partial z}(\rho_v q_G + \theta_G J_{hG}) + f_{LG}, \tag{1c}$$

where ρ_p (kg m^{-3}) is the phase or component mass density ($p = L, G, v$; for liquid, gas, and vapor), θ_p (m^3 m^{-3}) is the volumetric phase content, q_p (m s^{-1}) is the volumetric phase flux or specific discharge, J_{hG} (kg m^{-2} s^{-1}) is the gas-phase fluidodynamic dispersion flux, f_{LG} (kg m^{-3} s^{-1}) is the water transfer rate for evaporation from the liquid to the gas-phase per unit volume of the porous soil matrix, and finally, t (s) and z (m) are the time and the depth. Equations (1a), (1b), and (1c) correspond to the liquid-phase balance, the gas-phase balance, and the water vapor component balance, respectively [*Bear and Batchmat*, 1991; *Grifoll et al.*, 2005].

[4] *Grifoll et al.* [2005] compared their numerical simulation results with classical experimental data in the literature [*Jackson*, 1973; *Rose*, 1968a, 1968b] and found that soil-water and energy transport dynamics can be described without the use of empirical enhancing transport factors. Other authors have suggested that mechanical dispersion of

---

[1] Grup de Recerca DEW, Departament d'Enginyeria Quimica, Universitat Rovira i Virgili, Tarragona, Catalunya, Spain.

Corresponding author: J. Grifoll, Grup de Recerca DEW, Departament d'Enginyeria Quimica, Universitat Rovira i Virgili, 43007 Tarragona, Catalunya, Spain. (jordi.grifoll@urv.cat)

0043-1397/13/10.1002/wrcr.20105

water vapor should be considered [*Zeng et al.*, 2011a, 2011b], although not all of them included this mechanism in their own studies [*Novak*, 2010; *Smits et al.*, 2011].

[5] The simulation results of *Grifoll et al.* [2005] show that mechanical dispersion fluxes can account for a large proportion (up to 40%) of the total vapor flux. However, they do not identify the cause of the flow that creates this mechanical dispersion. In addition, they use a longitudinal dispersivity of 0.078 m to calculate the mechanical dispersion flux for a path of approximately 1 cm from the evaporation front to the soil surface. Although this dispersivity value was determined experimentally by *Biggar and Nielsen* [1976], the experimental conditions were very different to those of the simulated scenario, which could lead to a significant variation of the dispersivity values. In addition, dispersivity is known to be dependent on the length scale of measurement [*Gelhar et al.*, 1992], and there is a difference of at least 1 order of magnitude between the scale of the experimental system of *Biggar and Nielsen* [1976] and the scale of the system simulated by *Grifoll et al.* [2005].

[6] The first objective of this study is to identify and assess the gas-phase advection processes which can potentially induce a significant level of mechanical dispersion. The second objective is to analyze the sensitivity of evaporation flux to the numerical dispersivity value.

2. Dispersivity and Processes That Generate Gas Flow

[7] The fluidodynamic (hydrodynamic) dispersion flux in the gas phase J_{hG} comprises the mechanisms of diffusion and mechanical dispersion. These mechanisms are modeled according to *Bear and Bachmat* [1991] and using the following expression given by *Grifoll et al.* [2005] for a 1-D model:

$$J_{hG} = -\left(\frac{D_G}{\tau} + D_{mG}\right)\frac{\partial \rho_v}{\partial z}, \tag{2}$$

where D_G (m^2 s^{-1}) is the molecular diffusion coefficient for water vapor in air, τ is the gas-phase tortuosity, and D_{mG} (m^2 s^{-1}) is the mechanical dispersion coefficient for the gas phase. In the model by *Grifoll et al.* [2005], tortuosity is calculated by the first *Millington and Quirk* [1960] model, $\tau = \phi^{2/3}/\theta_G$, where ϕ is the porosity. For 1-D flows the mechanical dispersion coefficient can be estimated as

$$D_{mG} = \alpha_{lG}|v_G|, \tag{3}$$

where α_{lG} (m) is the longitudinal dispersivity, and $v_G = q_G/\theta_G$ (m s^{-1}) is the gas pore velocity.

[8] Under natural evaporation conditions, a receding drying front gradually forms within the soil, separating an upper zone (dry layer) close to the soil surface, where the liquid phase is practically absent, from a lower zone in which water can move, thanks to the higher liquid-phase saturation. In the dry layer, only gas-phase vapor-transport mechanisms help to transfer water vapor to the soil surface. These mechanisms are advection, diffusion, and mechanical dispersion. This latter is highly dependent on the value of dispersivity, which is subject to considerable uncertainty.

[9] Section 2.1 discusses the range of potential values for dispersivity in the dry layer. Sections 2.2–2.4 describe an order of magnitude study that compares D_G/τ and D_{mG} values in the dry layer for simple scenarios. The processes analyzed that could potentially generate gas flow and as a result mechanical dispersion are variation of temperature, variation of barometric pressure, and Stefan flow.

2.1. Soil Dispersivity Values

[10] According to equation (3), mechanical dispersion is directly proportional to dispersivity, so the selection of a representative dispersivity value is important when dispersion fluxes are simulated for mass transport in porous media.

[11] In the selection process, dispersivity can be regarded as a property of a medium [*Bear*, 1972], so it is only to be expected that dispersivity values for soils and aquifers will differ because their structural properties are substantially different [*Vanderborght and Vereecken*, 2007]. While a considerable amount of data is available on experimental groundwater dispersivity (see, for instance, the reviews by *Gelhar et al.* [1992] and *Schulze-Makuch* [2005]), the data available on water-saturated soils are scarcer. Early measurements of the leaching of water-soluble salts made by *Biggar and Nielsen* [1976] from their analysis of solute distribution at six depths between 0.305 and 1.824 m in natural fields resulted in a dispersivity of 0.078 m. A recent review of dispersivities for soils [*Vanderborght and Vereecken*, 2007] provides a database with 635 determinations in undisturbed soils under different experimental factors, including the travel distance. In the present study it is expected that the dry layer and thus the travel distances will be in the order of a few centimeters. The minimum travel distance reported in the database of *Vanderborght and Vereecken* [2007] is 0.05 m with 20 determinations, which are presented in the form of a histogram in Figure 1. Figure 1 shows that while dispersivities of 0.02 m or less are the most common, some values are above 0.05 m, and the maximum value reported was 0.128 m.

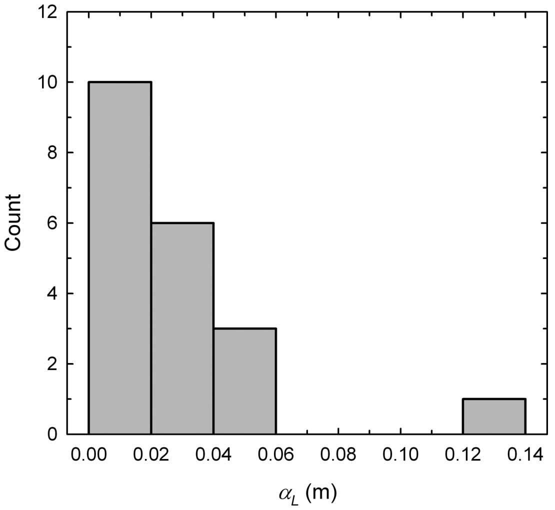

Figure 1. Histogram of the dispersivity values measured in undisturbed soils for a travel distance of 0.05 m as reported in the database of *Vanderborght and Vereecken* [2007].

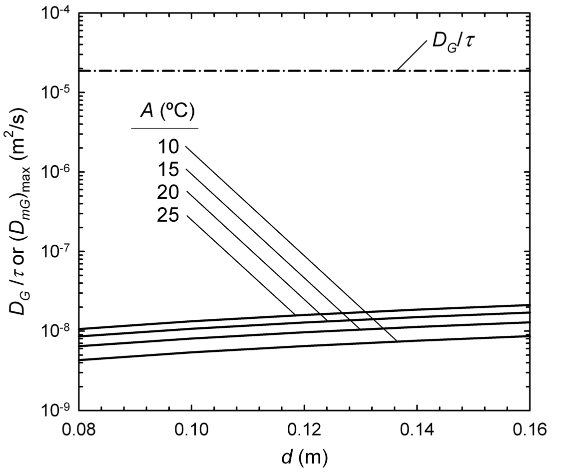

Figure 2. Comparison of the diffusion coefficient and the maximum mechanical dispersion coefficient caused by daily temperature variations.

[12] Theoretically, the dispersivities for gas- or liquid-phase saturation in the same porous matrix should be equivalent [*Bear*, 1972]; nevertheless, it seems that this equivalence has not been confirmed experimentally. It should also be noted that experimental dispersivity accounts for all transport mechanisms not explicitly identified or modeled, and which can change depending on whether the saturation phase is liquid or gas and on the physicochemical properties of the transported species. The amount of data available on gas-phase dispersivity is very limited [*Hamamoto et al*., 2009], and most of the recent data on artificial and homogeneous materials [*Gidda et al*., 2006; *Hamamoto et al*., 2009; *Sharma and Poulsen*, 2010; *Hibi et al*., 2012] are in the range 0.001–0.05 m already pointed out by *Costanza-Robinson and Brusseau* [2002].

[13] Some of the simulations presented in this study aim to elucidate which of the potential processes that can generate flow in the gas phase have mechanical dispersion fluxes that could be significant in the water evaporation process. To this end, the processes have been simulated, under different conditions but with a dispersivity value (0.078 m), well within the upper bound of the range determined experimentally. If a process does not generate appreciable mechanical dispersion under severe conditions, this mechanism can be safely neglected when the process is modeled, unless the expected conditions for the simulations are even more severe.

2.2. Temperature Variation

[14] Significant subsurface temperature fluctuations occur close to the soil surface. Since the gas-phase density is dependent on temperature, these fluctuations induce a flow. Under the assumptions that the porous medium resistance to the gas flow is negligible, that the medium is homogeneous, that the barometric pressure is constant, and that the gas phase behaves ideally, the number of gas moles per unit area of transversal surface between depth z and $z + \mathrm{d}z$ is given by

$$\mathrm{d}N(t,z) = \frac{P\theta_G}{R}\frac{\mathrm{d}z}{T(t,z)}, \tag{4}$$

where P (Pa) is the barometric pressure, R (Pa m^3 K^{-1} mol^{-1}) is the gas constant, and $T(t,z)$ (K) is temperature at depth z and time t. The variation in the number of gas moles along the soil column, due to temperature changes, generates a molar gas flux at the soil surface, which, when the volumetric gas-phase content is uniform, is given by

$$N''(t,0) = \frac{\mathrm{d}}{\mathrm{d}t}\int_0^\infty \mathrm{d}N(t,z) = \frac{P\theta_G}{R}\frac{\mathrm{d}}{\mathrm{d}t}\int_0^\infty \frac{\mathrm{d}z}{T(t,z)}. \tag{5}$$

[15] Considering that at the soil surface the temperature is $T(t,0)$, the pore gas velocity that crosses the soil surface is

$$v_G(t,0) = T(t,0)\frac{\mathrm{d}}{\mathrm{d}t}\int_0^\infty \frac{\mathrm{d}z}{T(t,z)}. \tag{6}$$

[16] Under the assumption that the soil surface temperature varies cyclically according to the expression

$$T(t,0) = \overline{T}_0 + A\sin(\omega t), \tag{7}$$

where $\overline{T}_0$ (K) is the average surface temperature, A (K) is the amplitude of the thermal oscillations, and ω is the radial frequency (s^{-1}), and considering soil heat transport only by conduction, the pseudostationary temperature as a function of time and depth is given as [*Hillel*, 1980]

$$T(t,z) = \overline{T}_0 + A\exp\left(-\frac{z}{d}\right)\sin\left(\omega t - \frac{z}{d}\right), \tag{8}$$

where d (m) is the damping depth, which depends on the thermal soil properties. For a sandy soil, $0.08 < d < 0.16$ m [*Hillel*, 1980]. Figure 2 shows the variation of the maximum mechanical dispersion coefficient $(D_{mG})_{\max}$ with d and A, which take values that cover most of the ranges for sandy soils under natural conditions. The value of $(D_{mG})_{\max}$ has been calculated according to equation (3) with $\alpha_{lG} = 0.078$ m, and the maximum value of v_G has been calculated according to equations (6) and (8) with $\overline{T}_0 = 293$ K. For comparison, Figure 2 also shows the effective diffusion coefficient (D_G/τ), which is invariant with respect to d and A. There is a difference of at least three orders of magnitude between the two vapor-transport coefficients, which suggests that under natural conditions the mechanical dispersion flux generated by temperature fluctuations is negligible compared to the diffusion flux.

2.3. Barometric Pressure Variation

[17] Barometric pressure variation causes air to be drawn upward and pushed downward in a process called *barometric pumping*. Barometric pressure variation is expressed as

$$P(t) = \overline{P}_0 + \Delta P\cos(\omega t), \tag{9}$$

where $\overline{P}_0$ (Pa) is the average barometric pressure, ΔP (Pa) is the amplitude, $\omega = 2\pi/\Gamma$ (s^{-1}), and Γ (s) is the characteristic period.

[18] Under the assumption that all soil properties are homogeneous to a depth L (m), where a gas-impermeable surface is located, the pore velocity at the soil surface is given by [*Auer et al*., 1996]

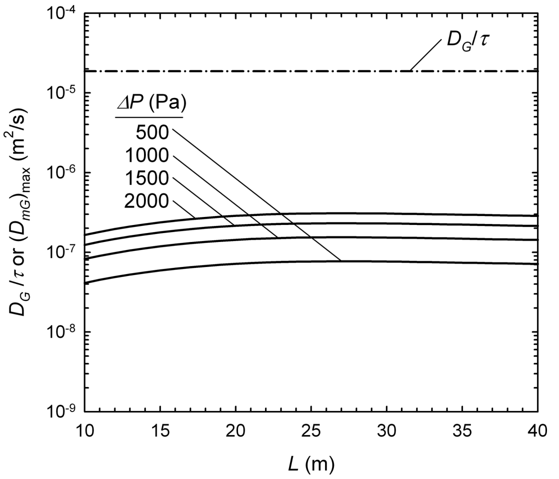

Figure 3. Comparison of the diffusion coefficient and the maximum mechanical dispersion coefficient caused by weekly barometric pressure variations. Soil properties: $K = 2.02 \times 10^{-13}$ m^2 and $\phi = 0.39$.

$$v_G(t,0) = -\mathrm{Re}\left\{\Delta P \frac{K}{\phi\mu} k \frac{\sinh\left(-kL\sqrt{i}\right)}{\cosh\left(kL\sqrt{i}\right)} \exp(i\omega t)\right\}, \qquad (10)$$

where $k^2 = \mu\phi 2\pi/(KP_0\Gamma)$, K (m^2) is the soil permeability, ϕ is the porosity, μ (Pa s) is the air viscosity, Re denotes the real part of a complex number, and i is the unit imaginary number.

[19] The mechanical dispersion coefficient has been calculated as the product of the longitudinal dispersivity (0.078 m), and the maximum value of $v_G(t,0)$ over the period Γ. Figure 3 shows the variation of $(D_{mG})_{\max}$ with respect to the depth L to the impermeable layer for $\Gamma = 7$ days and for a loam soil with the physical properties given by *Grifoll et al.* [2005] in their Case II ($K = 2.02 \times 10^{-13}$ m^2 and $\phi = 0.39$).

[20] Again, the diffusion coefficient is much higher than the mechanical dispersion coefficient. The difference is approximately two orders of magnitude, which suggests that atmospheric pumping cannot induce a significant dispersion flux. The same calculations were performed for characteristic periods in the range $1 < \Gamma < 10$ days with an amplitude $\Delta P = 2000$ Pa. Figure 4 shows the maximum mechanical dispersion coefficient at the soil surface attained for each period when the depth L was changed between 1 and 40 m. For each characteristic period Γ, Figure 4 also shows the depth at which this maximum is attained, L^*. When the period decreases, the maximum coefficient of mechanical dispersion increases, but even with a period as short as $\Gamma = 1$ day (at which the maximum dispersion is attained when the impermeable layer is located at $L^* = 10.5$ m), the diffusion coefficient is higher than the mechanical dispersion by more than one order of magnitude.

[21] It should be noted that the transport model proposed by *Grifoll et al.* [2005] does not include the barometric pressure variations, so this process cannot be the cause of the mechanical dispersion observed in their simulations.

2.4. Stefan Flow

[22] Stefan flow is a flow induced by the production or removal of chemical species at an interface, typically due to a phase transition or a chemical reaction. In stage 2 evaporation in soils, liquid water is available for evaporation at the drying front, located at some distance from the soil surface. Without taking mechanical dispersion into consideration, the water vapor generated at the drying front is transported toward the soil surface by two mechanisms: diffusion (i.e., the motion of vapor relative to the mass-average motion of the air-vapor mixture) and advection (i.e., the motion of vapor with the mass-average motion of the air-vapor mixture) [*Incropera et al.*, 2007; *Nellis and Klein*, 2009]. The production of vapor at the drying front induces this Stefan flow which, like any other flow in a porous matrix, is able to produce mechanical dispersion.

[23] To calculate the order of magnitude of the mechanical dispersion generated by this Stefan flow under stage 2 evaporation, a soil in which evaporation takes place with a flux E (m s^{-1}) is considered. In stage-two evaporation, this flux crosses the soil dry layer from the drying front to the surface and corresponds to a molar vapor flux N''_w (mol m^{-2} s^{-1}) given by

$$N''_w = E\frac{\rho_w}{M_w}, \qquad (11)$$

where ρ_w (kg m^{-3}) is the liquid water density, and M_w (kg mol^{-1}) is the molecular mass of water. Under the assumption of ideal gas behavior, the gas pore velocity close to the soil surface is given by

$$v_G = \frac{N''_w RT_0}{\phi P_0} = E\frac{\rho_w RT_0}{M_w \phi P_0}. \qquad (12)$$

[24] The mechanical dispersion coefficient generated by Stefan flow, calculated from equation (12) and $\alpha_{lG} = 0.078$

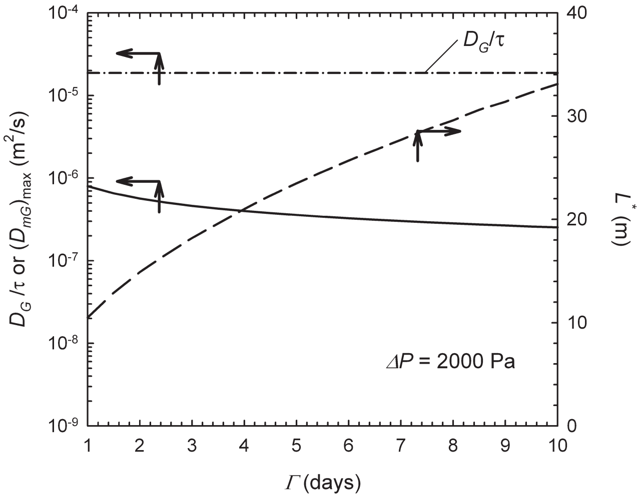

Figure 4. Comparison of the diffusion coefficient and the maximum mechanical dispersion coefficient caused by a cyclic barometric pressure variation with an amplitude $\Delta P = 2000$ Pa as a function of the characteristic period. Also, impermeable layer depth for which the maximum mechanical dispersion is attained (L^*) for each characteristic period. Soil properties: $K = 2.02 \times 10^{-13}$ m^2 and $\phi = 0.39$.

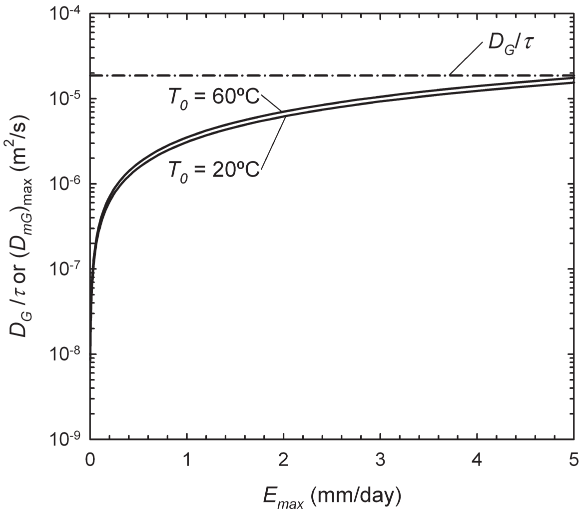

Figure 5. Comparison of the diffusion coefficient and the mechanical dispersion coefficient caused by Stefan flow.

m, and the effective diffusion coefficient are compared in Figure 5. The Stefan flow is estimated considering evaporation fluxes of up to 5 mm d^{-1} and for soil surface temperatures (T_0) of 60°C and 20°C under standard barometric pressure ($P_0 = 101{,}325$ Pa). At an evaporation flux of $E = 3$ mm d^{-1}, the gas-phase flow is high enough to generate a mechanical dispersion flux that accounts for 50% of the total vapor flux. It is worth noting that these fluxes should be considered as time point values, which differ from the daily average values.

[25] Comparison of Figures 2–5 suggests that under natural conditions the temperature and pressure perturbations do not generate gas fluxes that lead to appreciable mechanical dispersion, even for high longitudinal dispersivity values. In contrast, the Stefan flow generated by evaporation induces mechanical dispersion fluxes that can easily reach values comparable to those of the diffusion fluxes.

3. Sensitivity of Evaporation Flux to Dispersivity

[26] Once the process with the greatest potential to produce mechanical dispersion has been identified, we can examine the effect of the dispersivity value on the evaporation rate. In this section we again use the value $\alpha_{lG} = 0.078$ m as an upper bound for dispersivity, and a sensitivity analysis will show how the evaporation flux depends on α_{lG}. This analysis will be performed with the model given by *Grifoll et al.* [2005], which includes the mass balances given by equations (1a)–(1c). When these coupled mass balances are solved iteratively, equation (1b) provides the gas flux q_G along the soil column that results, among other dependencies, from the local evaporation rate (f_{LG}). The local values of q_G are used to compute the local values of the mechanical dispersion coefficient. So, although not explicitly stated by *Grifoll et al.*, [2005], the Stefan flow was implicitly included in equation (1b) when calculating q_G.

[27] The model is used to simulate the experimental study carried out by *Jackson* [1973] with the main hydraulic soil properties given as $K = 2.02 \times 10^{-13}$ m^2 and $\phi = 0.39$. Additional properties and climatological and geographical data can be found in *Grifoll et al.* [2005, Tables 1–3] for their Case II study. The numerical simulation results presented by these authors indicate that the model is able to describe the moisture variation at the soil surface, even in the presence of steep temperature and water content gradients, which develop naturally close to the soil surface.

[28] In the first simulation presented here (Case A), the dispersivity is set to $\alpha_{lG} = 0.078$ m. Figure 6 shows the evolution of temperature (Figure 6a), volumetric water

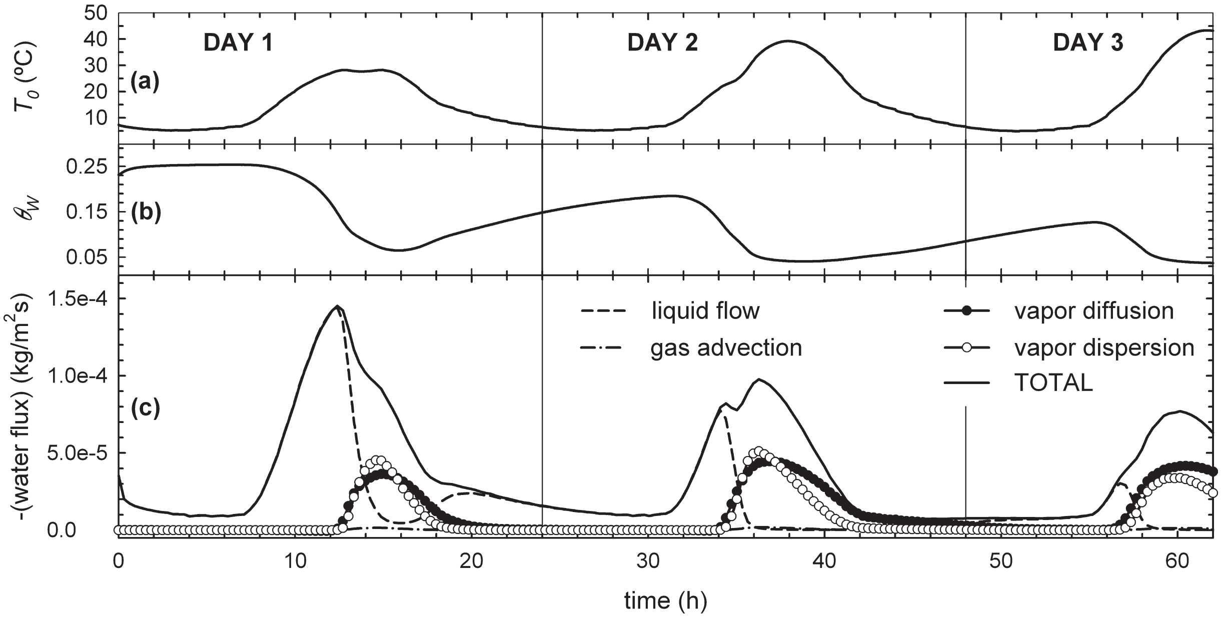

Figure 6. Evolution of (a) temperature, (b) volumetric water content, and (c) transport mechanisms at $z = 1$ mm for $\alpha_{lG} = 0.078$ m (Case A).

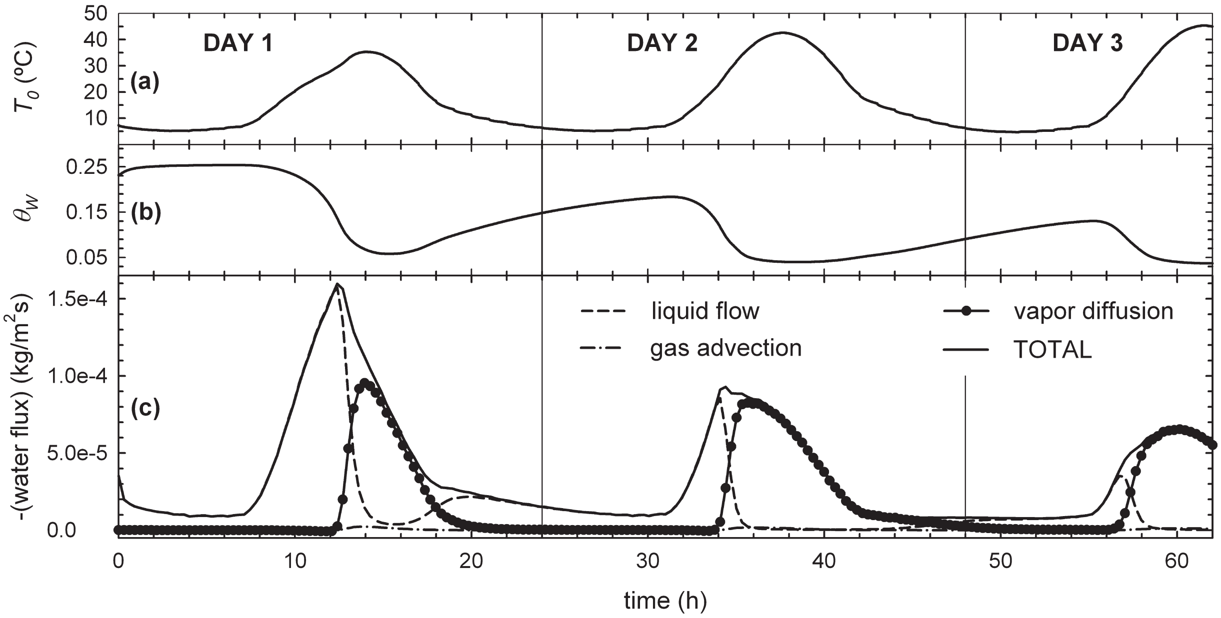

Figure 7. Evolution of (a) temperature, (b) volumetric water content, and (c) transport mechanisms at $z = 1$ mm for $\alpha_{IG} = 0.0$ m (Case B).

content (Figure 6b), and transport mechanisms (Figure 6c) at a depth of 1 mm over a period of 62 h, starting with the initial conditions given by *Grifoll et al.* [2005]. Both temperature and volumetric water content are shown to vary cyclically, with an overall tendency for temperature to increase and for water content to decrease.

[29] Figure 6c shows how the contribution of each mechanism to the total evaporation flux varies during the experiment. Analysis of this evolution reveals that the mechanisms behave in a complementary fashion. When one mechanism ceases to contribute, another or various mechanisms take over, smoothing the evolution of the evaporation flux. For instance, in the middle part of the first day, the liquid water flow toward the surface decreases rapidly and cannot contribute to the evaporation process. As soon as this occurs, diffusion and dispersion mechanisms take over and remain active until the evening, at which point they are replaced again by liquid flow. It is interesting to highlight that during the central period of both the first and second days, the evaporation flux rises and generates a mechanical dispersion flux that exceeds the diffusion flux for a few hours. The maximum mechanical dispersion flux falls significantly each day due to a reduction in gas flow caused, in turn, by the overall decrease in the evaporation flux. Over the same period, the maximum daily diffusion flux barely changes because it is not influenced directly by the evaporation flux.

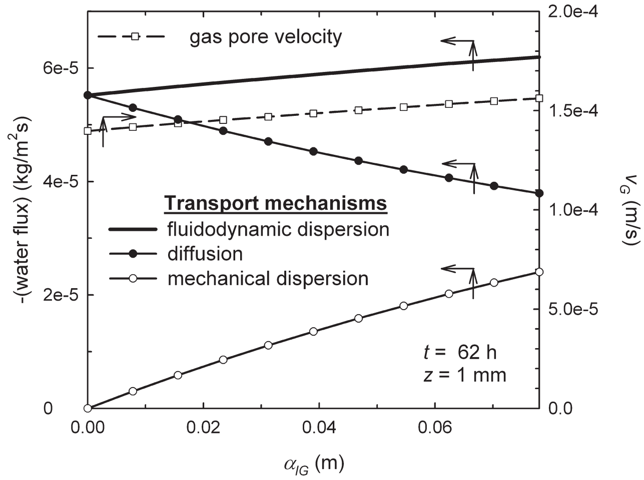

Figure 8. Variation of the fluidodynamic dispersion flux as well as its components, diffusion, and mechanical dispersion, with dispersivity ($t = 62$ h and $z = 1$ mm). Also, gas pore velocity at the same position and time.

[30] A second simulation (Case B) was performed with a dispersivity value $\alpha_{IG} = 0.0$ m, and all other parameters had the same values as in Case A. Figure 7 shows the variation of temperature, volumetric water content, and vapor flux at a depth of 1 mm with the contribution of each mechanism. Comparison of Figures 6 and 7 shows that the temperature and volumetric water content dynamics are very similar in Cases A and B, which suggests that the dispersivity value has a negligible effect on the overall process. This behavior is consistent with the findings of *Hanks and Gardner* [1965], who pointed out that evaporation in a drying soil under stage 2 is limited by the ability of the mechanisms that drive the liquid water up to the drying front. Vapor-transport resistance from the front to the surface layer is much less than liquid transport resistance, so it is the latter that largely governs the evaporation process.

[31] An examination of the contribution of each vapor-transport mechanism, shown in Figure 7c, explains why the process exhibits low sensitivity to dispersivity. In Case B, in the absence of mechanical dispersion flux, the diffusion flux increases significantly and largely offsets the mechanical dispersion flux calculated in Case A. This happens

because the evaporation front during the middle part of the day has a slightly higher temperature than in Case A, which increases the vapor pressure, the vapor concentration gradient, and therefore the diffusion flux.

[32] To analyze the effects of the dispersivity value on the diffusion and dispersion fluxes, several simulations of the same case were performed with dispersivities that varied between 0.0 and 0.078 m. Taken from these simulations, Figure 8 shows the mechanical dispersion and diffusion fluxes, as well as the sum of the two (the fluidodynamic dispersion flux), at a depth of $z = 1$ mm after 62 h of evolution (which corresponds to the final simulation time in Cases A and B). The increase in dispersivity from 0.0 to 0.078 m leads to an increase of only 12% in the fluidodynamic dispersion flux. However, the diffusion flux is 46% higher with no mechanical dispersion than for $\alpha_{lG} = 0.078$ m.

[33] Therefore, Figure 8 clearly illustrates the complementary action of diffusion and mechanical dispersion. When the mechanical dispersion is decreased in the model, the numerical solution shifts to counteract the imposed change, increasing the diffusion flux by a degree that compensates for a significant proportion of the transport previously carried out by mechanical dispersion. This observation suggests that in numerical simulations of natural systems using mechanistic models for nonisothermal transport in soils, evaporation flux, temperature, and other macroscopic variables are highly insensitive to the numerical value of dispersivity. Also for the same simulations, Figure 8 shows the gas pore velocities at $t = 62$ h and $z = 1$ mm obtained when α_{lG} varied between 0.0 and 0.078 m. Gas pore velocity is simultaneously responsible for the vapor advection flux, as accounted for by the $\rho_v q_G$ term in equation (1c), and the dispersion flux, as given in the same equation by the term $\theta_G J_{hG}$ which includes dispersion as indicated in equations (2) and (3). For the transport conditions found in the different simulations given in Figure 8, fluidodynamic dispersion in the gas phase is for all practical purposes, the only active process that drives the vapor flow toward the soil surface. As a consequence, gas pore velocity and fluidodynamic dispersion are almost proportional, as Figure 8 indicates.

4. Conclusions

[34] This study shows that the mechanical dispersion of water vapor in soils under natural conditions could make a significant contribution to the total vapor transport in the evaporation process. Of the three gas flow processes analyzed in this study: (a) temperature variation, (b) barometric pumping, and (c) Stefan flow, only the latter can generate a significant mechanical dispersion flux within the order of magnitude of diffusion.

[35] Numerical simulations of a natural evaporation scenario with different dispersivity values show that mechanical dispersion and diffusion behave in a complementary way. When the mechanical dispersion flux decreases due to a reduction in the dispersivity value, diffusive transport increases and compensates for the decrease in mechanical dispersion to a large extent.

[36] **Acknowledgments.** This research was funded with grants DPI2012-35687 and CTQ2008-05758/PPQ (Spanish Government) and 2009SGR-01529 (Generalitat de Catalunya Government, Catalonia, Spain). I thank Joan Rosell-Llompart for his constructive suggestions. Comments by M. D. Novak and other referees helped to improve the final version.

References

Auer, L. H., N. D. Rosenberg, K. H. Birdsell, and E. M. Whitney (1996), The effects of barometric pumping on contaminant transport, *J. Contam. Hydrol.*, *24*, 145–166.

Bear, J. (1972), *Dinamics of Fluids in Porous Media*, Dover, New York.

Bear, J., and Y. Bachmat (1991), *Introduction to Modeling of Transport Phenomena in Porous Media*, Kluwer, Dordrecht, Netherlands

Biggar, J. W., and D. R. Nielsen (1976), Spatial variability of the leaching characteristics of a field soil, *Water Resour. Res.*, *12*(1), 78–74.

Costanza-Robinson, M. S., and M. L. Brusseau (2002), Gas phase advection and dispersion in unsaturated porous media, *Water Resour. Res.*, *43*, W02414, doi:10.1029/2005WR004474.

Gelhar, L. W., C. Welty, and K. R. Rehfeldt (1992), A critical review of data on field-scale dispersion in aquifers, *Water Resour. Res.*, *28*(7), 1955–1974.

Gidda, T., D. Cann, W. H. Stiver, and R. G. Zytner (2006), Air flow dispersion in unsaturated soil, *J. Contam. Hydrol.*, *82*, 118–132.

Grifoll, J., J. M. Gastó, and Y. Cohen (2005), Non-isothermal soil water transport and evaporation, *Adv. Water Resour.*, *28*, 1254–1266.

Hamamoto, S., P. Moldrup, K. Kawamoto, T. Komatsu, and D. E. Rolston (2009) Unified measurement system for the gas dispersion coefficient, air permeability, and gas diffusion coefficient in variably saturated soil, *Soil Sci. Soc. Am. J.*, *73*(6), 1921–1930.

Hanks, R. J., and H. R. Gardner (1965), Influence of different diffusivity-water content relations on evaporation of water from soils, *Soil Sci. Soc. Am. Proc.*, *29*(5), 495–498.

Hibi, Y., Y. Kanou, and Y. Ohira (2012) Estimation of mechanical dispersion and dispersivity in a soil-gas system by column experiments and the dusty gas model, *J. Contam. Hydrol.*, *131*, 39–53.

Hillel, D. (1980), *Fundamentals of Soil Physics*, Academic, San Diego, Calif.

Ho, C. K., and S. W. Webb (1998), Review of porous media enhanced vapor-phase diffusion mechanisms, models, and data—Does enhanced vapor-phase diffusion exist?, *J. Porous Media*, *1*, 71–92.

Incropera, F. P., D. P. DeWitt, T. L. Bergman, and A. S. Lavine (2007), *Fundamentals of Heat and Mass Transfer*, 6th ed., pp. 886–889, Wiley, Hoboken, N. J.

Jackson, R. D. (1973), *Diurnal changes in soil-water content during drying. In* Field Soil Water Regime, edited by R. R. Bruce et al., pp. 37–55, Soil Sci. Soc. Am., Madison, Wis.

Millington, R. J., and J. P. Quirk (1960), Transport in porous media, in *Transactions of the 7th International Congress of Soil Science Society, vol. 1, Madison, Wis.*, edited by F. A. van Beren et al., pp. 97–107, Elsevier, Amsterdam.

Nellis, G., and S. Klein (2009), *Heat Transfer*, pp. E23-15–E23-18, Cambridge Univ. Press, Cambridge.

Novak, M. D. (2010), Dynamics of the near-surface evaporation zone and corresponding effects on the surface energy balance of a drying bare soil, *Agric. For. Meteorol.*, *150*, 1358–1365.

Philip, J. R., and D. A. deVries (1957), Moisture movement in porous materials under temperature gradients, *Trans. Am. Geophys. Union*, *38*, 222–231.

Rose, C. W. (1968a), Water transport in soil with a daily temperature wave: I. Theory and experiment, *Aust. J. Soil Res.*, *6*, 31–44.

Rose, C. W. (1968b), Water transport in soil with a daily temperature wave: II. Analysis, *Aust. J. Soil Res.*, *6*, 45–57.

Schulze-Makuch, D. (2005), Longitudinal dispersivity data and implications for scaling behavior, *Ground Water*, *43*(3), 443–456. doi:10.1111/j.1745-6584.2005.0051.x.

Sharma, P., and T. Poulsen (2010), Gas dispersion and immobile gas content in granular porous media: Effect of particle size nonuniformity, *Soil Sci.*, *175*, 426–431, doi:10.1097/SS.0b013e3181f0edaf.

Shokri, N., P. Lehmann, and D. Or (2009), Critical evaluation of enhancement factors for vapor transport through unsaturated porous media, *Water Resour. Res.*, *45*(10), W10433, doi:10.1029/2009WR007769.

Smits, K. M., A. Cihan, T. Sakaki, and T. H. Illangasekare (2011), Evaporation from soils under thermal boundary conditions: Experimental and modeling investigation to compare equilibrium and non-equilibrium based approaches, *Water Resour. Res.*, *47*, W05540, doi:10.1029/2010WR009533.

Šimůnek, J., M. Šejna, H. Saito, M. Sakai, and M. Th. van Genuchten Genuchten (2008), *The HYDRUS-1D software package for simulating the one-dimensional movement of water, heat, and multiple solutes in variably-saturated media, Version 4.0*, Univ. of Calif. Riverside, Riverside.

Vanderborght, J., and H. Vereecken (2007), Review of dispersivities for transport modeling in soils, *Vadose Zone J.*, *6*(1), 29–52, doi:10.2136/vzj2006.0096.

Zeng, Y., Z. Su, L. Wan, and J. Wen (2011a), Numerical analysis of air-water-heat flow in unsaturated soil: Is it necessary to consider airflow in land surface models?, *J. Geophys. Res.*, *116*, D20107, doi:10.1029/2011JD015835.

Zeng, Y., Z. Su, L. Wan, and J. Wen (2011b), A simulation analysis of the advective effect on evaporation using a two-phase heat and mass flow model, *Water Resour. Res.*, *47*, W10529, doi:10.1029/2011WR010701.